INFECTION AND IMMUNITY, Apr. 2008, p. 1628–1638 Vol. 76, No. 4
0019-9567/08/$08.00+0 doi:10.1128/IAI.01393-07

Vibrio vulnificus Biotype 2 Serovar E *gne* but Not *galE* Is Essential for Lipopolysaccharide Biosynthesis and Virulence▽

Esmeralda Valiente,[1] Natalia Jiménez,[2] Susana Merino,[2] Juan M. Tomás,[2] and Carmen Amaro[1]*

Universidad de Valencia Departamento de Microbiología y Ecología, c/ Dr. Moliner, 50, Burjasot, Valencia,[1] and Universidad de Barcelona Departamento de Microbiología, Diagonal 645, 08071 Barcelona,[2] Spain

Received 17 October 2007/Returned for modification 10 December 2007/Accepted 21 January 2008

This work aimed to establish the role of *gne* (encoding UDP-GalNAc 4-epimerase activity) and *galE* (encoding UDP-Gal-4-epimerase activity) in the biosynthesis of surface polysaccharides, as well as in the virulence for eels and humans of the zoonotic serovar of *Vibrio vulnificus* biotype 2, serovar E. DNA sequence data revealed that *gne* and *galE* are quite homologous within this species (≥90% homology). Mutation in *gne* of strain CECT4999 increased the surface hydrophobicity, produced deep alterations in the outer membrane architecture, and resulted in noticeable increases in the sensitivity to microcidal peptides (MP), to eel and human sera, and to phagocytosis/opsonophagocytosis. Furthermore, significant attenuation of virulence for eels and mice was observed. By contrast, mutation in *galE* did not alter the cellular surface, did not increase the sensitivity to MP, serum, or phagocytosis, and did not affect the virulence for fish and mice. The change in the attenuated-virulence phenotype produced by a mutation in *gne* was correlated with the loss of the O-antigen lipopolysaccharide (LPS), while the capsule was maintained. Complementation of a *gne*-deficient mutant restored the LPS structure together with the whole virulence phenotype. In conclusion, *gne*, but not *galE*, is essential for LPS biosynthesis and virulence in the zoonotic serovar of *V. vulnificus* biotype 2.

Vibrio vulnificus is a pathogenic bacterial species that occurs in warm aquatic environments with intermediate levels of salinity. It is commonly isolated in temperate, subtropical, and tropical areas, where it is a risk to public health. *V. vulnificus* is able to infect fish and humans and causes a disease called vibriosis (41). Human vibriosis occurs after infection of preexisting wounds with seawater, after an individual is injured while fishing or handling fish, or after ingestion of raw seafood (41). Fish vibriosis is produced after gill or intestine colonization, without previous injury (19, 37). Human and fish vibriosis can lead to septicemia and death if innate defenses do not act properly and in time, which makes the mechanisms of resistance of *V. vulnificus* to innate defenses a key virulence factor in septicemia. Classically, the human virulent strains are classified in biotypes 1 and 3, while the fish virulent strains are classified in biotype 2 (11, 53). Interestingly, some biotype 2 strains, which are serologically homogeneous, are able to infect both humans and fish (3). These strains are designated serovar E strains (VSE strains) and are distributed worldwide. Recently, the genomes of two strains of *V. vulnificus* biotype 1 isolated from human blood in Asia have been described and compared (15, 29). Both of these strains are serologically different from VSE strains (unpublished results).

A number of virulence factors that confer resistance to human innate immunity have been described for biotype 1 strains. Two such factors are the capsule that protects bacteria from phagocytosis (58) and an iron acquisition system that depends on vulnibactin, which is used for sequestering iron from host transferrin (28). In VSE strains, the capsule seems not to be essential for resistance to eel serum since spontaneous translucent variants survive in fresh eel serum (10), while the lipopolysaccharide (LPS) could contribute to this resistance since spontaneous O-antigen mutants that develop rugose colonies are sensitive to eel serum and are avirulent (2).

No information concerning either the chemical structure of cell surface polysaccharides or the genes involved in their biosynthesis in *V. vulnificus* VSE strain cells is available, although several genes, such as *wbpO*, *wbpP*, and *wza*, have recently been described in *V. vulnificus* biotype 1 (46, 47, 59). *wbpO* encodes a putative UDP-*N*-acetyl-D-galactosamine dehydrogenase essential for LPS biosynthesis, *wbpP* encodes a putative UDP-*N*-acetylglucosamine 4-epimerase essential for capsule biosynthesis, and *wza* encodes a sugar transferase also needed for capsule biosynthesis. In other bacterial species, additional genes, such as *gne* (encoding UDP-*N*-acetylgalactosamine [UDP-GalNAc] 4-epimerase activity) and *galE* (encoding UDP-galactose [UDP-Gal] 4-epimerase activity), have been described as genes that are involved in LPS or capsule biosynthesis and virulence (12, 16).

The objective of the present work was to establish the roles played by *gne* and *galE* in the biosynthesis of surface polysaccharides, as well as in the virulence for fish and humans, in the zoonotic serovar of *V. vulnificus* biotype 2. To this end, we looked for both of these genes in the previously published genome of biotype 1 strain YJ016, performed PCR to determine whether they were present in representative VSE strains, and obtained two mutants from a selected VSE strain by allelic exchange. The selected strain was CECT4999, originally isolated from a diseased eel, which is highly virulent for both eels and mice (an animal model used to test human virulence) and is resistant to both eel and human sera. We demonstrated that mutations in *gne* alter the O antigen of the LPS but not the capsule. The *gne*-deficient mutant showed significant attenua-

* Corresponding author. Mailing address: Departamento de Microbiología y Ecología, Universidad de Valencia, c/ Dr. Moliner, 50, Burjasot, Valencia, Spain. Phone: 34 96 354 31 04. Fax: 34 96 354 45 70. E-mail: carmen.amaro@uv.es.

▽ Published ahead of print on 28 January 2008.

tion of virulence for mice and eels, but the *galE*-deficient mutant did not show significant attenuation.

MATERIALS AND METHODS

Bacterial strains, plasmids, and growth conditions. Bacterial strains and plasmids used in this work are shown in Table 1. *V. vulnificus* strains were grown in tryptic soy broth containing 1% NaCl (TSB-1), on tryptic soy agar containing 1% NaCl (TSA-1), in marine seawater yeast extract (MSWYE), on MSWYE agar (42), and in M9 minimal medium (50) supplemented with 10 mM $MgSO_4$, 10 mM $CaCl_2$, and 20% Casamino Acids (Difco) at 28°C for 24 h. For enzymatic determinations, the strains were cultured in Davis minimal medium (13) with 0.2% glucose (DMM-glu) or galactose (DMM-gal) as the only carbon source. *Escherichia coli* and *Salmonella enterica* serotype Typhimurium strains were grown in Luria-Bertani broth and on Luria-Bertani agar at 37°C for 24 h. When required, ampicillin (Amp) (100 μg ml^{-1}), rifampin (Rif) (100 μg ml^{-1}), or chloramphenicol (Cm) (20 μg ml^{-1}) was added to the different media. All the strains were stored in TSB-1 with or without an antibiotic plus dimethyl sulfoxide at −80°C. All bacterial counts were obtained by using the drop plate methodology (26).

General DNA methods, DNA sequencing, and computer analysis of sequence data. General DNA manipulations were performed as previously described (50). DNA restriction endonucleases, T4 DNA ligase, *E. coli* DNA polymerase (Klenow fragment), and alkaline phosphatase were used as recommended by the suppliers. Double-stranded DNA sequencing was performed by using the dideoxy chain termination method (50) with an ABI Prism dye terminator cycle sequencing kit (Perkin-Elmer). Oligonucleotides were purchased from Pharmacia LKB Biotechnology. The DNA sequence was translated in open reading frames with the Frameplot program (27) and was compared with DNA sequences from the nonredundant GenBank (National Center for Biotechnology Information) and EMBL (European Biotechnology Information Service) databases by using the BLAST network service (1). ClustalW was used for multiple-sequence alignment.

DNA amplification and plasmid and mutant construction. The VV3026 and VV2639 genes of biotype 1 strain YJ016 (accession number BA000037) were selected for primer design to detect putative *gne* and *galE* genes in VSE cells due to their homology to *gne* and *galE* of *Aeromonas hydrophila* AH-3 (12) (Fig. 1). The primers used for *gne* amplification were *gne* for (5′-TTTCAGTTCGTCAG CCACC-3′) and *gne* rev (5′-TCAGCAATATCACCGGCAC-3′), which resulted in a 531-bp amplicon; and the primers used for *galE* amplification were *galE* for (5′-TGACATTCGTGACGAAGCC-3′) and *galE* rev (5′-TCCCCACCGATTT CAATGC-3′), which resulted in a 584-bp amplicon. These amplicons were subcloned as incomplete copies (with an internal sequence missing both the 5′ and 3′ ends) of the *gne* and *galE* genes in the vector pGEMT, creating pGEMT-*gne* and pGEMT-*galE*. After EcoRI digestion of plasmids pGEMT-*gne* and pGEMT-*galE*, the gel-purified DNA was treated with *E. coli* DNA polymerase I (Klenow fragment) to create blunt ends in order to ligate the band to pCM100 (suicide plasmid, λpir dependent) and obtain plasmids pCM100-*gne* and pCM100-*galE*. Plasmids pCM100-*gne* and pCM100-*galE* were used to obtain *gne*- and *galE*-deficient mutants from CECT4999 by a single recombination event using previously described procedures (50). To this end, pCM100-*gne* and pCM100-*galE* were isolated, transformed into *E. coli* MC1061-λ*pir* (12), and transferred by triparental conjugation to strain CECT4999-0 (a spontaneous rifampin-resistant [Rif^r] mutant) as previously described (12). The Cm^r Rif^r transconjugants should have contained the mobilized plasmid integrated into the chromosome by homologous recombination, leading to two incomplete copies of the *gne* and/or *galE* gene (defined insertion mutants). Complementation analysis of the different VSE mutants was performed by conjugal transfer of wild-type complete *galE* and *gne* genes cloned in pGEMT to the corresponding mutants. Recombinants were selected on TSA-1 containing Cm, Rif, and Amp. Additional transformation experiments with pGEMT-*gne* and pGEMT-*galE* were performed with strains DH5α (which naturally lacks UDP-GalNAc 4-epimerase activity) (23) and SL1306 (a mutant that lacks UDP-Gal 4-epimerase activity) (54).

Cell extract production and measurement of enzymatic activity (UDP-Gal 4-epimerase and UDP-GalNAc 4-epimerase assays). Suspensions of bacteria (25%, wt/vol) that were washed in 25 mM Tris-HCl buffer (pH 7.5) containing 1 mM $MgCl_2$ were disrupted with a Branson model 350 Sonifier at 0°C. The disrupted bacteria were subjected to high-speed centrifugation (180,000 × *g* for 2 h) at 5°C to obtain cell extracts. Protein concentrations of extracts were determined by using the Bio-Rad Bradford assay as recommended by the manufacturer with bovine serum albumin as the standard.

The assays for UDP-Gal 4-epimerase and UDP-GalNAc 4-epimerase activities were performed as previously described (17, 57). For UDP-Gal 4-epimerase, the initial rates of NADH formation were determined by using the kinetics program installed in the spectrophotometer (Beckman DU640). A molar extinction coefficient (E_{340}) of 6.220 M^{-1} cm^{-1} was assumed for all calculations. For UDP-GalNAc 4-epimerase, the conversion of UDP-GalNAc to UDP-*N*-acetylglucosamine (GlcNAc) was measured after acid hydrolysis by the 3.6-fold-greater absorbance at 585 nm (A_{585}) of free GlcNAc than of GalNAc in the Morgan-Elson reaction. Following hydrolysis and completion of the Morgan-Elson reaction, color development was measured at 585 nm. Control assays with extract and with only substrate were performed simultaneously. All assays were performed in triplicate. Product formation (i.e., formation of GlcNAc by hydrolysis of UDP-GlcNAc) was measured using standard plots prepared by subjecting UDP-GlcNAc, UDP-GalNAc, GlcNAc, and GalNAc (Sigma-Aldrich, St. Louis, MO) to the same procedures.

Electron microscopy. To stain flagella, cell suspensions were mixed with 2% phosphotungstic acid (pH 7) and air dried. Ultrastructural studies of the bacterial envelopes were performed by using ruthenium red staining for polysaccharides as described by Biosca et al. (10). Briefly, agar pieces with bacteria were placed into sodium cacodylate buffer (0.2 M, pH 7.2) containing 2.5% glutaraldehyde plus 0.075% ruthenium red, washed with sodium cacodylate buffer, and incubated for 2 h at 4°C in 1% osmium tetroxide. Then samples were washed in ultrapure MilliQ water, dehydrated using a graded ethanol series (30 to 100% ethanol, 10 min per step), and transferred sequentially into 3:1, 1:1, and 1:3 ethanol-epoxy resin (Aname) for 1 h per step and finally into 100% resin overnight. Then samples were embedded in flat silicone molds and placed inside a 60°C oven to polymerize for 2 days. Blocks were removed from the molds, and 100-nm ultrathin sections were obtained using a Leica Ultracut R ultramicrotome (Leica Microsystems, Milton Keynes, England). Observations were made with a JEOL 1010 transmission electron microscope.

MICs of microcidal peptides (MP) and human transferrin. Stationary-phase bacteria were suspended in phosphate-buffered saline (pH 7) containing 1% NaCl (PBS-1) at a concentration of approximately 10^7 CFU ml^{-1}, and 10 μl was inoculated into MSWYE plates containing polymyxin B sulfate (500 to 10^5 U ml^{-1}; Sigma), poly-L-lysine (30 to 300 μg ml^{-}; Sigma), or transferrin (2.5 to 50 μM; Sigma) and incubated for 24 h at 28°C. The MIC endpoint was defined as the lowest antibiotic concentration at which there were no visible colonies. Experiments were carried out in triplicate.

Antigen extraction, separation, and visualization. Outer membrane proteins (OMP) were obtained from cells after sonication and differential solubilization of the inner membranes in a Sarkosyl solution (0.05%) as described by Biosca et al. (9). The extracellular proteins (ECP) were obtained after separation by differential centrifugation from cells grown on cellophane sheets covering TSA-1 plates using the protocol of Liu (34). OMP and ECP concentrations of samples were determined by the method of Lowry et al. (35). Crude fractions of bacterial polysaccharides (LPS and capsule) were obtained from cell lysates after proteinase K digestion (Boehringer Mannheim) as described by Hitchcock and Brown (25). The LPS concentration was determined with ProQ Emerald 300 staining for glycoproteins (Invitrogen) by following the manufacturer's instructions. OMP, ECP, LPS, and capsule antigens were separated and examined by sodium dodecyl sulfate-polyacrylamide gel electrophoresis (30) in discontinuous gels (4% stacking gel, 12% separating gel). Protein bands were visualized by Coomassie brilliant blue staining, and LPS and capsule bands were visualized by immunostaining after transfer from the polyacrylamide gels to nitrocellulose sheets (0.45 μm; Bio-Rad) as described by Towbin et al. (55). Blotting was done at 200 mA for 2 h in Tris-glycine-methanol transfer buffer (25 mM Tris, 192 mM glycine [pH 8.3], 20% [vol/vol] methanol). Immunostaining was performed with previously obtained serovar-specific sera (4) (dilution for immunostaining, 1:1,000) or with the same sera after absorption with one of the mutants. The absorption process involved incubating serum with mutant cells (1×10^9 CFU per ml in PBS-1) with gentle shaking for 30 min at 37°C, followed by filtration through 0.22-μm-pore size membranes (Millipore filters) (43). Absorbed sera were diluted 1:10 for immunostaining (43).

Eel serum, mucus, and phagocyte collection. Humoral (serum and gill mucus) and cellular (head kidney, spleen, and blood phagocytes) defensive factors were obtained from adult eels (*Anguilla anguilla*) as described by Esteve-Gassent et al. (18) and Castro et al. (14), respectively. For the cellular factors, the head kidney and spleen were aseptically removed and crushed, and blood was taken from the caudal vein; these factors were mixed (1:3) with Leibovitz's medium (L-15) (Gibco) containing 2% fetal calf serum, heparin (10 IU ml^{-1}), penicillin (100 IU ml^{-1}), and streptomycin (100 μg ml^{-1}), layered onto a 34 to 51% (vol/vol) Percoll gradient, and centrifuged at 400 × *g* for 30 min at 4°C. The interface cells were collected, washed twice, and suspended at a concentration of 1×10^6 viable

TABLE 1. Bacterial strains and plasmids used in this work

Strain or plasmid	Origin, genotype, and/or phenotype	Reference(s) or source
Vibrio vulnificus strains		
Biotype 1		
YJO16	Isolated from human blood in Taiwan, avirulent for eels, virulent for mice, genome sequenced, opaque morphotype	15, 32
Biotype 2 serovar A		
CECT5768	Isolated from diseased eel in Spain, virulent for eels, avirulent for mice, opaque morphotype	21
CECT7030	Isolated from diseased eel in Denmark, virulent for eels, virulence for mice not tested, opaque morphotype	21
Biotype 2 serovar E		
CECT4999	Isolated from kidney of diseased eel in Spain, virulent for mice and eels, opaque morphotype	51
CECT4864	Isolated from kidney of diseased eel in Spain, virulent for mice and eels, opaque morphotype	51
CCUG38521	Isolated from human wound in Sweden, virulent for mice and eels, opaque morphotype	51
CECT4866 (= ATCC 33817)	Isolated from human wound in United States, virulent for mice and eels, opaque morphotype	3
CECT5763	Isolated from seawater in Spain, virulent for mice and eels, OM	51
4999-0	CECT4999, spontaneous Rif^r, opaque morphotype	This study
4999-1[a]	CECT4999, spontaneous translucent variant	This study
4999-2	CECT4999 (pCM100-*gne*), Rif^r Cm^r, opaque morphotype, *gne*-deficient mutant	This study
4999-3	CECT4999 (pCM100-*galE*), Rif^r Cm^r, opaque morphotype, *galE*-deficient mutant	This study
C4999-2	R99-2 with pGEMT-*gne*, opaque morphotype, complemented strain	This study
C4999-3	R99-3 with pGEMT-*galE*, opaque morphotype, complemented strain	This study
Biotype 2 serovar I[b]		
95-8-6	Isolated from diseased eel in Denmark, virulent for eels, virulence for mice not tested, opaque morphotype	51
95-8-161	Isolated from diseased eel in Denmark, virulent for eels, virulence for mice not tested, opaque morphotype	51
Biotype 3		
11028	Isolated from human wound in Israel, avirulent for eels, virulent for mice, opaque morphotype	11
Escherichia coli strains		
XL1-Blue	*endA1 recA1 hsdR17 supE44 thi-1 gyrA96 relA1 lac* [F′ *proAB lacI*^{q}*ZΔM15* Tn*10* cTet^r)]	Stratagene
DH5α	F$^-$ *endA hsdR17* (r_K^- m_K^+) *supE44 thi-1 rexA1 gyrA96* ϕ80*lacZ*	23
MC1061-λ*pir*	*thi thr-1 leu-6 proA2 his-4 argE2 lacY1 galK2 ara-14 xyl-5 supE44*	49
S. enterica serotype Typhimurium strains		
SL3770	Expresses smooth LPS	54
SL1306	*galE503*, produces rough LPS of Rc chemotype	54
Plasmids		
pGEM-T Easy	PCR cloning vector, Amp^r	Promega
pCM100	pGP704 suicide plasmid, λ*pir* dependent, Cm^r	61
pCM100-*gne*	pCM100 with an internal fragment of *gne*, Cm^r	This study
pCM100-*galE*	pCM100 with an internal fragment of *galE*, Cm^r	This study
pGEMT-*gne*	pGEMT with the complete *gne* gene of CECT4999, Amp^r	This study
pGEMT-*galE*	pGEMT with the complete *galE* gene of CECT4999, Amp^r	This study

[a] Strain obtained by passage to laboratory media as described by Biosca et al. (10).
[b] Strains previously identified as serotype O3 and O3/O4 (38) and reclassified as serovar I (C. Amaro, unpublished results).

cells ml^{-1} in the same medium. Viability was estimated by the trypan blue exclusion test. Cell suspensions were immediately used in phagocytosis assays.

Colonization assays. (i) Motility. Motility was measured by transferring bacterial colonies on MSWYE into motility medium (1% tryptone, 0.5% yeast extract, 1% NaCl) supplemented with 0.3% (swimming) and 0.6% (swarming) agar. Halo diameters were measured after 24 h of incubation at 28°C.

(ii) Chemotaxis. Serum and mucus from eels, as well as human serum (Sigma), were used as substrates. Chemotaxis was evaluated using the capillary assay

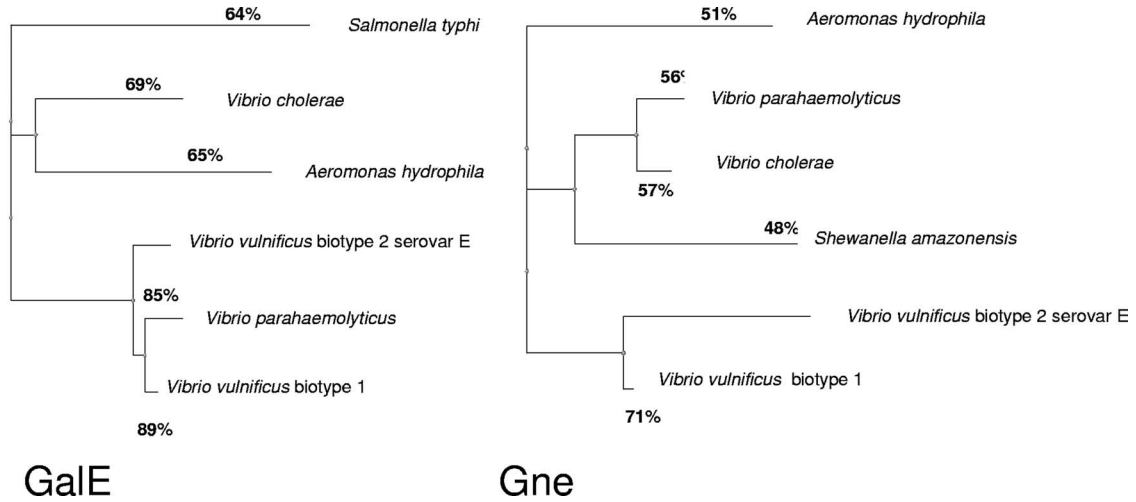

FIG. 1. Dendrogram showing the amino acid sequence relatedness of *V. vulnificus* GalE and Gne with UDP-glucose 4-epimerases of other vibrios and related species using the TreeView software (45).

described by Larsen et al. (31). To equalize differences in random motility and experimental variations, the chemotactic responses were expressed as the ratio of the number of bacteria in attractant capillaries to the number of bacteria in control capillaries filled with chemotaxis buffer.

(iii) Adherence to mucus. Ninety-six-well microtiter plates covered with eel mucus were inoculated with 100 μl of a bacterial suspension (10^3 to 10^4 CFU ml^{-1}) in PBS-1 per well, incubated at 28°C for 24 and 72 h and 1 and 2 weeks, washed three times with distilled water, stained with a 0.1% crystal violet solution, washed twice, and destained with 95% alcohol. The optical density at 540 nm was determined with a spectrometer (Termospectronic Helios λ).

(iv) Cell surface hydrophobicity. Hydrophobicity was measured by the salt aggregation test (SAT) using ammonium sulfate solutions (0, 0.01, 0.05, 0.1, 0.5, 1, 2, and 4 mol $liter^{-1}$) (33).

(v) Biofilm formation. Cells were grown in MSWYE (42). Biofilm formation was evaluated as described by O'Toole and Kolter (44) by determining the ability of cells to adhere to polystyrene tubes (hydrophobic surface) or glass tubes (hydrophilic surface). The tubes were incubated at 28°C for 5 and 10 h. Biofilm formation was quantified by addition of 200 μl of 95% (vol/vol) ethanol to crystal violet-stained samples, and the absorbance at 540 nm was determined with a plate reader (Multiskan Askcent; Labsystems).

Eel complement fixation assay. Anti-sheep red blood cell (SRBC) (Biomedics) serum (anti-SRBC serum) was obtained by injecting an SRBC suspension (5% in PBS-1) plus Freund's incomplete adjuvant (1:1) into eels using the protocol of Esteve-Gassent et al. (18). After 2 weeks, anti-SRBC serum was collected and inactivated by heating it at 56°C 30 min. The assay was performed on 96-well microtiter plates as follows. One hundred microliters of inactivated anti-SRBC serum was added to 100 μl of a 5% SRBC solution in 0.01 M EDTA (tetrasodium salt)-gelatin-Veronal buffer (EDTA-GVB^{2+}), and the mixture was incubated for 30 min at 28°C to sensitize the SRBC. Then 200-μl aliquots of the bacterial suspensions in PBS-1 were added to 200 μl of nonimmune eel serum, incubated at 28°C for 1 h, and centrifuged (400 × *g*, 5 min, 4°C). The supernatants serially diluted in EDTA-GVB^{2+} (1:100 to 1:51,200) were added either to 100 μl of sensitized SRBC (1:1) to calculate 50% hemolysis due to complement activated by the classical pathway (CH_{50}) or to nonsensitized SRBC to calculate 50% hemolysis due to complement activated by the alternative pathway (ACH_{50}) after incubation at 28°C for 2 h and assessment of the relative hemoglobin content by determination of the optical density at 540 nm with a microplate reader (Bio-Rad). Experiments were done in triplicate. A complement fixation index (CFI) was calculated by determining the ACH_{50} or CH_{50} ratio before and after bacterial incubation (60).

Resistance to phagocytosis and opsonophagocytosis by eel phagocytes. To obtain opsonized bacteria, a bacterial suspension containing 10^8 CFU ml^{-1} in PBS-1 was incubated with 10% nonimmune serum for 30 min. Then the bactericidal activity of eel phagocytes was determined as previously described (52), with some modifications. Briefly, eel leukocytes (10^7 cells ml^{-1} in Hanks balanced salt solution) were dispensed into Eppendorf plates and incubated with opsonized and nonopsonized bacteria (100 μl). After 0, 1, 2, 3, and 4 h of incubation, 50 μl of saponin (0.15% in distilled water; Sigma) was added to each well, and the microplates were incubated for 15 min at 4°C to lyse the cells. Bacterial survival was measured both by determining bacterial culturability on TSA-1 plates and by determining bacterial viability by reduction of 3-(4, 5-dimethylthiazol-2-yl)-2,5-diphenyltetrazolium bromide (MTT). For the latter assay, a solution of MTT (2 mg ml^{-1} in distilled water) was added (50 μl per well), and plates were incubated for 15 min. MTT reduction was measured with a multiscan spectrophotometer (Bio-Rad) at a wavelength of 630 nm. A bactericidal index was determined by dividing the absorbance/count for each sample by the absorbance/count for the control. Experiments were performed in triplicate.

Resistance to serum and mucus. Fresh gill mucus from eels, fresh and heat-inactivated (56°C for 60 min) human serum, and fresh and heat-inactivated (56°C, 30 min) eel serum were used in resistance assays (2, 36). A suspension containing 10^3 to 10^4 CFU ml^{-1} in PBS-1 was mixed with serum mucus samples, and the mixtures were incubated at 28°C (for eels) or 37°C (for humans) for 4 h. Viability counting was performed on TSA-1 plates at zero time and after 4 h of incubation.

Virulence for fish and mice. Virulence was determined by calculating the 50% lethal dose (LD_{50}) by the method of Reed and Muench (48), using elvers (average weight, 10 g) and BALB/c mice (average weight, 20 g). The elvers were kept in a 60-liter fiberglass tank containing freshwater at 26°C with a filtration and recirculation system. Groups of six fish and six mice were inoculated intraperitoneally with 0.1 and 0.2 ml, respectively, of serial 10-fold dilutions of bacteria in PBS-1 as previously described (5, 6), and mortality was recorded daily for a 7-day period. Mortality was considered to be caused by *V. vulnificus* only if the inoculated bacterium was recovered in pure culture from internal organs (5, 6).

Statistical assays. One-way analysis of variance using the Tukey test was used to evaluate the significance of differences in assays and was performed with the GraphPad Prism program (version IV). Values were considered significantly different if the *P* value was <0.05. Experiments were performed in triplicate.

Nucleotide sequence accession numbers. The nucleotide sequence accession number for the VSE *gne* region described in this paper is EU041623, and the nucleotide sequence accession number for the *galE* region is EU041622.

RESULTS

Cloning, sequence analysis, and isolation of *gne* and *galE* mutants. Two genes (annotated VV2639 and VV3026) with high levels of homology to the *A. hydrophila* epimerase genes *galE* and *gne* (12) were found in the genome of human-pathogenic *V. vulnificus* biotype 1 strain YJ016. All DNA samples from the *V. vulnificus* strains shown Table 1 were positive for the *gne* and *galE* genes in a PCR assay. The coding region of *galE* of CECT4999 was 1,020 nucleotides long and showed

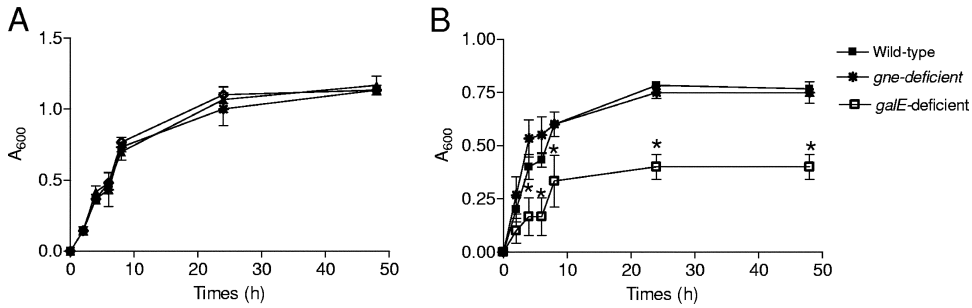

FIG. 2. Growth curves in TSB-1 (A) and DMM-gal (B) of strain CECT4999 and its derivatives, the *gne*-deficient mutant (4999-2) and the *galE*-deficient mutant (4999-3), incubated at 28°C. An asterisk indicates that a value is significantly different from the value for the wild-type strain (CECT4999) ($P < 0.05$).

92% homology to VV2639, while the coding region of *gne* was 849 nucleotides long and showed 90% homology to VV3026. The deduced amino acid sequence revealed that *galE* codes for a protein containing 339 amino acids with 89% homology to the VV2639 protein and 65% homology to GalE of *A. hydrophila*, while *gne* codes for a protein containing 282 amino acids with 71% homology to the VV3026 protein and 51% homology to Gne of *A. hydrophila* (Fig. 1). *galE* and *gne* did not show significant homology to *wpbO*, *wpbP*, or *wza* of *V. vulnificus* biotype 1.

In order to isolate deficient mutants of strain CECT4999, two plasmids that carried 584- and 531-bp DNA fragments corresponding to incomplete copies of *galE* and *gne*, respectively, were constructed. Rif- and Cm-resistant isolates were confirmed by Southern blot hybridization with appropriate DNA probes and were used to obtain insertion mutants.

Enzymatic activities and growth curves. Figure 2 and Table 2 show growth curves in rich and minimal media and epimerase activities for the wild-type strain and its derivatives. The curves for the wild-type and mutant strains were statistically similar in TSB-1 and DMM-glu and different in DMM-gal (Fig. 2). In DMM-gal, the generation time of the *galE*-deficient mutant was twice the generation time of the wild-type strain and the *gne*-deficient mutant and the maximum population size of the *galE*-deficient mutant was threefold less than the maximum population size of the wild-type strain and the *gne*-deficient mutant, which suggests that mutations in *galE* significantly reduce but do not eliminate the ability of the bacteria to grow with galactose as the sole carbon source (Fig. 2). In fact, the wild-type strain and the *galE*-deficient mutant showed both epimerase activities, although the UDP-Gal 4-epimerase activity was lower in the mutant (significant difference, $P < 0.05$) (Table 2). In contrast, the *gne*-deficient mutant completely lacked UDP-GalNAc 4-epimerase activity and had UDP-Gal 4-epimerase activity in DMM-glu or DMM-gal that was not significantly different from that of the wild-type strain (Table 2). *E. coli* strain DH5α, which lacks UDP-GalNAc 4-epimerase activ-

TABLE 2. UDP-Gal 4-epimerase and UDP-GalNAc 4-epimerase activities in *V. vulnificus* wild-type and mutant cell extracts

Strain	Carbon source[a]	UDP-Gal 4-epimerase activity (nmol min^{-1} mg^{-1})[b]	UDP-GalNAc 4-epimerase activity (nmol min^{-1} mg^{-1})[c]
CECT4999 (wild type)	Glucose	78.3 ± 1.1	20.6 ± 0.8
	Galactose	32.6 ± 1.0	11.9 ± 1.2
4999-2 (*gne* mutant)	Glucose	75.8 ± 1.5	<0.08[d,e]
	Galactose	31.5 ± 1.3	<0.08[d,e]
4999-3 (*galE* mutant)	Glucose	16.7 ± 2.1[f]	20.1 ± 0.5
	Galactose	12.8 ± 1.4[f]	11.1 ± 1.6
C4999-2 (pGEMT-*gne*)	Glucose	76.0 ± 1.8	21.6 ± 1.2
	Galactose	30.4 ± 1.9	10.7 ± 2.3
C4999-3 (pGEMT-*galE*)	Glucose	77.3 ± 1.7	20.8 ± 1.4
	Galactose	30.9 ± 2.2	11.7 ± 0.8
E. coli DH5α	Glucose	NT[g]	<0.08[d,e]
E. coli DH5α (pGEMT-*gne*)	Glucose	NT	8.4 ± 0.9
E. coli DH5α (pGEMT-*galE*)	Glucose	NT	<0.08[d,e]
SL3770 (wild type)	Glucose	63.5 ± 2.8	<0.09[d,e]
SL1306 (*galE* mutant)	Glucose	<0.05[d,e]	<0.09[d,e]
SL1306 (pGEMT-*gne*)	Glucose	12.8 ± 0.6	7.9 ± 1.2
SL1306 (pGEMT-*galE*)	Glucose	56.1 ± 1.4	<0.09[d,e]

[a] Each strain was grown in DMM-glu (containing 0.2% glucose) or DMM-gal (containing 0.2% galactose).
[b] Nanomoles of UDP-Gal converted to UDP-Glc per minute per milligram of protein.
[c] Nanomoles of UDP-GalNAc converted to UDP-GlcNAc per minute per milligram of protein.
[d] No detectable activity.
[e] Significantly different from the value for the wild-type strain ($P < 0.001$).
[f] Significantly different from the value for the wild-type strain ($P < 0.05$).
[g] NT, not tested.

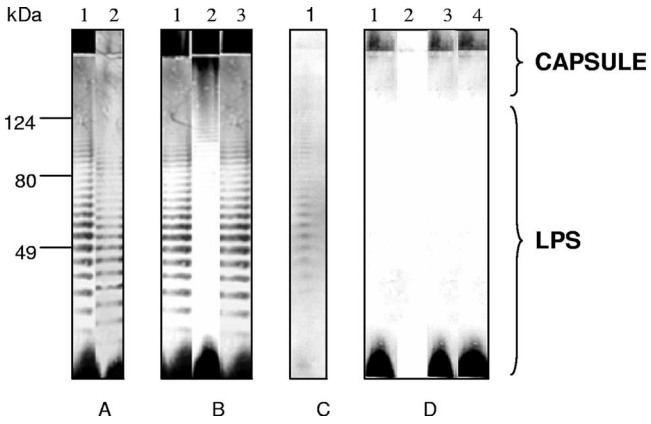

FIG. 3. Immunostaining of LPS and capsule extracts with (A) rabbit anti-CECT4999 serum diluted 1:1,000 (lane 1, CECT4999; lane 2, 4999-1 [translucent variant]), (B) rabbit anti-CECT4999 serum diluted 1:1,000 (lane 1, 4999-3 [*galE*-deficient mutant]; lane 2, 4999-2 [*gne*-deficient mutant]; lane 3, C4999-2 [*gne*-complemented strain]), (C) rabbit anti-CECT4999 serum after absorption of the antibodies with 4999-2 cells (anti-O-antigen serum) diluted 1:10 (lane 1, CECT4999), and (D) rabbit anti-CECT400 serum after absorption with 4999-1 cells (anticapsule serum) diluted 1:10 (lane 1, CECT4999; lane 2, 4999-1; lane 3, 4999-3; lane 4, 4999-2).

ity, had UDP-GalNAc 4-epimerase activity after complementation with *gne* but not after complementation with *galE* (Table 2). Moreover, *S. enterica* serotype Typhimurium SL1306, which is not able to grow on DMM-gal and shows no detectable UDP-Gal 4-epimerase activity (54) (Table 2), grew on this medium and displayed this epimerase activity after complementation with pGEMT-*gne* or pGEMT-*galE* (Table 2). Finally, complementation of the *V. vulnificus gne*-deficient mutant with pGEMT-*gne* and complementation of the *galE*-deficient mutant with pGEMT-*galE* restored the wild-type phenotype.

Surface antigens. Colonies of the wild-type strain, the *gne*-deficient mutant, and the *galE*-deficient mutant on TSA-1 were opaque and had similar degrees of opacity, whereas colonies of strain 4999-1 were translucent. No apparent differences in the OMP and ECP patterns were observed among the strains (data not shown). In contrast, some differences in polysaccharides were detected among the strains (Fig. 3). Thus, after immunostaining of LPS-capsule extracts with anti-serovar E antibodies, the wild-type strain and the *galE*-deficient mutant showed the same pattern, which corresponded to the pattern for a smooth LPS plus the capsule (Fig. 3A and B). The translucent variant contained the whole LPS and lacked most of the capsular material, especially the part corresponding to the diffuse slowly migrating band that did not enter the separating gel (Fig. 3A), and the *gne*-deficient mutant lacked most of the LPS bands (Fig. 3B). After immunostaining of the wild-type strain with serum absorbed with the *gne*-deficient mutant, only the O antigen was observed (Fig. 3C), confirming that *gne* affected LPS; and after immunostaining with serum absorbed with the translucent variant, only the highest-molecular-weight portion of the capsule was stained (Fig. 3D). As Fig. 3D shows, the *gne*- and *galE*-deficient mutants were encapsulated. Electron micrographs of ruthenium red-stained ultrathin sections with capsule staining are shown in Fig. 4. Wild-type and mutant strains were surrounded by an electron-dense layer located outside the outer membrane (OM), which was apparently more dispersed or absent in the translucent variant (Fig. 4). The OM of the wild-type strain, the translucent variant, and the *galE*-deficient mutant had the same appearance; however, the OM of the *gne*-deficient mutant was profoundly altered, and there was a concomitant increase in the periplasmic space, which was filled with electron-dense material (Fig. 4). Complementation of the *gne*-deficient mutant with pGEMT-*gne* restored the whole structure of LPS (Fig. 3B), as well as the architecture of the OM (Fig. 4), whereas complementation of the *galE*-deficient mutant with pGEMT-*galE* did not alter either the OM architecture or the antigenic phenotype, which were identical to those of the wild-type (Fig. 4 and data not shown).

Hydrophobicity and biofilm formation. There were significant differences between strains in surface hydrophobicity, measured by determining the lowest molarity of ammonium

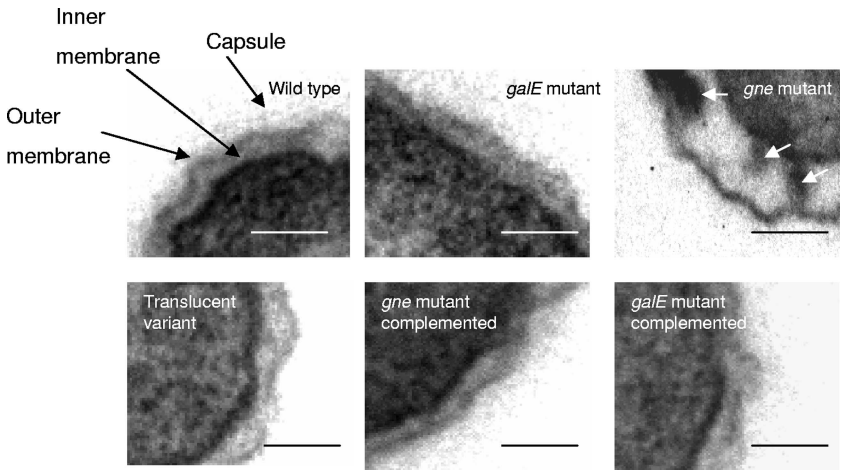

FIG. 4. Electron micrographs of strains CECT4999, 4999-3 (*galE*-deficient mutant), 4999-2 (*gne*-deficient mutant), 4999-1 (translucent variant), C4999-2 (*gne*-complemented strain), and C4999-3 (*galE*-complemented strain) after ruthenium red staining of ultrathin sections. The white arrows indicate the electron-dense periplasmic material. Bars = 0.1 μm.

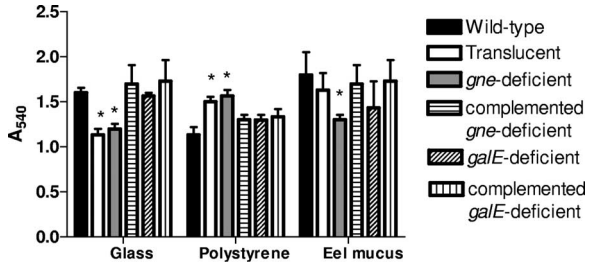

FIG. 5. Biofilm formation by CECT4999 and its derivatives on glass, polypropylene, and eel mucus measured by determining the absorbance at 540 nm (Multiskan Askcent; Labsystems). The strains used were strains CECT4999 (wild-type strain), 4999-1 (translucent variant), 4999-2 (*gne*-deficient mutant), 4999-3 (*galE*-deficient mutant), C4999-2 (*gne*-complemented strain), and C4999-3 (*galE*-complemented strain). An asterisk indicates that the value is significantly different from the value for the wild-type strain ($P < 0.001$).

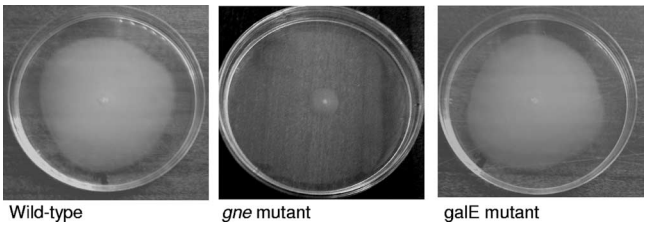

FIG. 6. Swimming behavior of strains CECT4999 (wild-type strain), 4999-2 (*gne*-deficient mutant), and 4999-3 (*galE*-deficient mutant).

sulfate at which the cells agglutinated (SAT assay) ($P < 0.05$). The SAT value for the wild-type and *galE*-deficient strains was 4 mol liter^{-1}, whereas the SAT value for the translucent variant and the *gne*-deficient mutant was 0.5 mol liter^{-1}. In accordance with the SAT values, the latter strains formed more biofilm on hydrophobic surfaces (polystyrene), whereas the wild-type and *galE*-deficient strains formed more biofilm on hydrophilic surfaces (glass) (significant differences, $P < 0.05$) (Fig. 5). When biofilm formation on eel skin mucus was examined, the *gne*-deficient mutant formed less biofilm than the wild-type strain (significant difference, $P < 0.05$), and the *galE*-deficient mutant did not differ significantly from the wild-type strain (Fig. 5). Complementation of the *gne*-deficient mutant with pGEMT-*gne* completely restored the hydrophobicity and biofilm formation patterns, whereas complementation of the *galE*-deficient mutant with pGEMT-*galE* did not alter the surface and adhesive properties (Fig. 5).

Chemotaxis and motility. Large amounts of CECT4999 and mutant bacteria accumulated in capillaries containing eel mucus compared with control capillaries containing chemotaxis buffer. The strains also showed positive chemotaxis toward both eel and human sera, and there were no significant difference between strains. Motility assays revealed that the swimming and swarming halo diameters exhibited by the wild-type strain, the translucent variant, and the *galE*-deficient mutant were not significantly different (diameters for swimming, 10 ± 1 mm; diameters for swarming, 11.0 ± 0.5 mm) and were greater than those of the *gne*-deficient mutant (diameters for swimming, 5.0 ± 0.3 mm; diameters for swarming, 6.0 ± 0.5 mm). Figure 6 shows the swimming behavior of the strains. Complementation of the *gne*-deficient mutant with *gne* increased the swimming and swarming halo diameters to the wild-type strain values. Both the wild-type strain and the mutants, including the *gne*-deficient mutant, possessed polar flagella with apparently similar lengths and widths.

Resistance to eel innate immunity. (i) Resistance to mucus and serum and sensitivity to MP and human serum transferrin. All the strains grew in gill mucus (Table 3). The wild-type strain and the *galE*-deficient mutant were also resistant to eel and human serum, whereas the translucent variant was resistant to eel serum and sensitive to human serum and the *gne*-deficient mutant was sensitive to both sera. The bactericidal effect of human serum on the translucent variant was partially eliminated by heat inactivation; however, the bactericidal effects of human and eel sera on the *gne*-deficient mutant were maintained even after heat inactivation (Table 3).

All strains were able to fix the eel complement activated by both pathways, regardless of cell viability (Table 3). There were no significant differences in CFI values between the wild-type strain and the *galE*-deficient mutant, which fixed more complement when it was activated by the alternative pathway (Table 3). By contrast, the translucent variant and the *gne*-deficient mutant fixed more complement than the other two strains (significant differences, $P < 0.05$) and showed similar values for CFI (no significant differences) regardless of the route of complement activation (Table 3).

The translucent variant and the *gne*-deficient mutant were more sensitive to the selected MP than the wild-type strain (significant differences, $P < 0.05$), and the most sensitive strain was the *gne*-deficient mutant (Table 3). The MICs of MP for the *galE*-deficient mutant were similar to those of the wild-type strain (Table 3). Resistance to MP, as well as to human and eel sera, was reestablished in the *gne*-deficient mutant by complementation with pGEMT-*gne* (Table 3). Finally, the MIC of human transferrin was the same for all strains (20 mM).

(ii) Resistance to phagocytosis and opsonophagocytosis. Eel phagocytes were able to ingest *V. vulnificus* cells regardless of whether they were opsonized by serum complement (Fig. 7), although a significant increase in the average number of ingested bacteria per phagocyte (from two bacteria to five bacteria) was detected when bacteria were opsonized. Bacterial survival after 1, 3, and 5 h of incubation with eel phagocytes was analyzed. The MTT and cultivability data were similar, and only data for cultivable bacteria recovered after phagocytosis are shown in Fig. 7. The wild-type strain and its derivatives, the translucent variant, and the *galE*-deficient mutant resisted the killing mechanisms of eel phagocytes, and there were no significant differences in bacterial survival (Fig. 7). In contrast, the *gne*-deficient mutant was sensitive to both phagocytosis and opsonophagocytosis. Thus, the survival percentage compared with the wild-type strain decreased from 1 to 3 h of incubation (significant differences, $P < 0.05$) for phagocytosis and opsonophagocytosis (Fig. 7).

Virulence for mice and eels. The LD_{50}s for mice and eels of the wild-type strain and its derivatives are shown in Table 3. The LD_{50}s of the *galE*-deficient mutant were similar to the LD_{50}s of the wild-type for both eels and mice (Table 3). However, the *gne*-deficient mutant was avirulent for eels and showed a significant reduction in virulence for mice, and the

translucent variant also showed a significant reduction in virulence for both hosts (Table 3). Complementation with pGEMT-*gne* completely restored the virulence for fish or mice (the LD_{50}s were similar to those of the wild-type strain) in the *gne*-deficient mutant, while no changes were observed in the *galE*-deficient mutant after complementation with and pGEMT-*galE* (Table 3).

DISCUSSION

This work aimed to establish the role of *gne* and *galE* in the biosynthesis of surface polysaccharides, as well as in virulence for eels and humans of the zoonotic serovar of *V. vulnificus* biotype 2. Putative homologues of these genes were first identified in the genome of the human-pathogenic *V. vulnificus* biotype 1 isolate YJ016 and were amplified and sequenced in the VSE isolate CECT4999. The sequences of VSE strain genes (*galE* and *gne*) were highly similar (90 to 92%) to the sequences of their homologs in biotype 1 strain YJ016. In addition, both genes were found by PCR in all *V. vulnificus* isolates tested regardless of biotype and serovar.

The enzymatic analyses performed with the mutants and the complemented strains, including the analyses performed with the complemented *E. coli* and *S. enterica* serovar Typhimurium strains, confirmed that *gne* encodes an epimerase with UDP-GalNAc 4-epimerase activity that is responsible for the conversion of UDP-GalNAc to UDP-GlcNAc and that *galE* encodes a protein with UDP-Gal 4-epimerase activity that is responsible for the conversion of UDP-Gal to UDP-Glc. In addition, the experiments performed with *Salmonella* suggest that *gne* encodes an epimerase with both UDP-GalNAc and UDP-Gal activities. In accordance with this observation, the *V. vulnificus gne* mutant exhibited only a very small reduction in the UDP-Gal 4-epimerase activity, probably because the main enzyme activity is due to GalE. At the same time, the reduced UDP-Gal 4-epimerase activity observed for the *V. vulnificus galE* mutant is supported by the fact that Gne can have reduced UDP-Gal 4-epimerase activity compared to GalE (Table 2). A similar situation has been described in *A. hydrophila* (12) and *Campylobacter jejuni* (8), in which Gne exhibits double activity as a UDP-GalNAc 4-epimerase and a UDP-Gal 4-epimerase and could supply the function of GalE. These results contrast with the results obtained for *E. coli* and *S. enterica* serovar Typhimurium, in which the GalE protein is the only UDP-Gal 4-epimerase (54). In these enterobacteria, mutations in *galE* are correlated with changes in the LPS chemical structure produced by an O-antigen-deficient LPS (54). In addition, *gne* and *galE*, as well as the putative proteins that they encode, were highly homologous to *Aeromonas gne* and *galE* genes and proteins, respectively, suggesting that the two genes could correspond to *gne* and *galE* and could encode UDP-GalNAc 4-epimerase and UDP-Gal 4-epimerase activity, respectively. *V. vulnificus* VSE *gne* and *galE* do not show significant homology with the recently described gene *wbpP*, which codes for a UDP-GlcNAc epimerase essential for capsule biosynthesis in biotype 1 strains (47).

The *gne*-deficient mutant had profound alterations in the cellular envelope that were visible by electron microscopy. Thus, the OM displayed irregular morphology, limiting the enlarged periplasmic space, in which electron-dense material

TABLE 3. Survival in serum and mucus, CFI, and MICs of transferrin, lysozyme, and cationic peptides as well as virulence of *V. vulnificus* strains

Strain	Survival index[a]					CFI with live cells[b]		MICs			Virulence (LD_{50})	
	Eel serum		Human serum		Eel mucus (gills)							
	NIS	I-NIS	NIS	I-NIS		ACH_{50}	CH_{50}	Lysozyme (mg ml^{-1})	Polymyxin B (IU ml^{-1})	Polu-L-lysine (μg ml^{-1})	Eels	Mice
CECT4999 (wild type)	50 ± 8	47 ± 6	57 ± 7	51 ± 5	49 ± 5	6.0 ± 0.5	4.8 ± 0.3	>100	5,000	150	1.7×10^2	4.2×10^6
4999-1 (translucent)	39 ± 5[c]	40 ± 7[c]	0[d]	20 ± 4[c]	43 ± 6	6.9 ± 0.5[c]	6.8 ± 0.3[c]	10[d]	500[d]	50[c]	2×10^{4c}	9.7×10^{7c}
4999-2 (*gne* deficient)	0[d]	0[d]	0[d]	0[d]	44 ± 3	7.0 ± 0.7[c]	7.0 ± 0.6[c]	10[d]	300[d]	50[c]	$>10^{7d}$	8.5×10^{7c}
4999-3 (*galE* deficient)	46 ± 7	43 ± 6	53 ± 5	54 ± 5	48 ± 4	6.1 ± 0.4	4.6 ± 0.5	100	1,000	100	2×10^2	7×10^6
C4999-2 (4999-2 complemented)	48 ± 9	45 ± 7	53 ± 5	48 ± 7	50 ± 6	NT[e]	NT	100	1,000	150	3×10^2	6.7×10^6
C4999-3 (4999-3 complemented)	52 ± 9	51 ± 5	54 ± 5	50 ± 6	49 ± 4	NT	NT	100	5,000	150	2×10^2	4.5×10^6

[a] The survival index is the ratio of the final bacterial count to the initial bacterial count. NIS, fresh nonimmune serum; I-NIS, inactivated nonimmune serum.
[b] The CFI of eel complement is expressed as the ACH_{50} or CH_{50} ratio before and after bacterial incubation.
[c] The value is significantly different from the value for the wild-type strain ($P < 0.05$).
[d] The value is significantly different from the value for the wild-type strain ($P < 0.001$).
[e] NT, not tested.

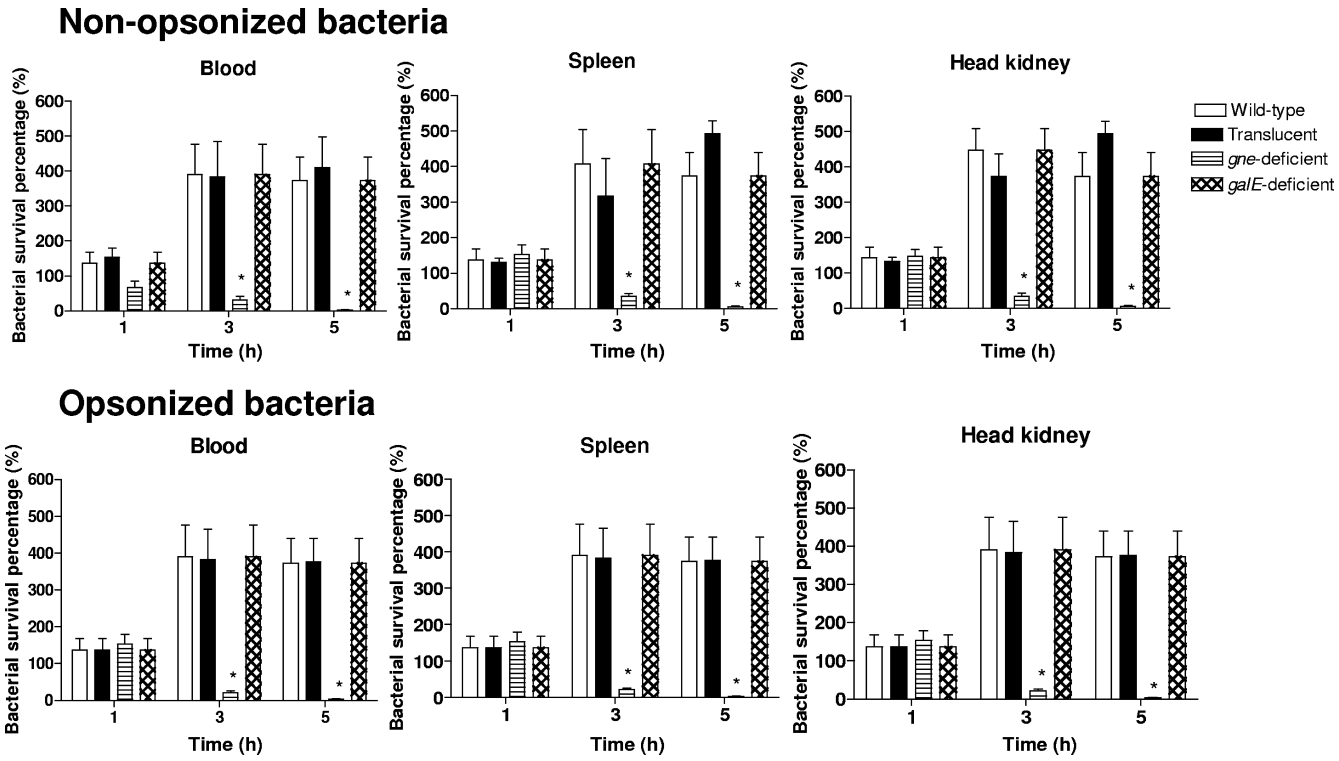

FIG. 7. Bactericidal activity of phagocytes from spleen, blood, and head kidney against nonopsonized or opsonized VSE strains. The strains used were strains CECT4999 (wild-type strain), 4999-1 (translucent variant), 4999-2 (*gne*-deficient mutant), 4999-3 (*galE*-deficient mutant), C4999-2 (*gne*-complemented strain), and C4999-3 (*galE*-complemented strain). An asterisk indicates that the value is significantly different from the value for the wild-type strain ($P < 0.001$).

accumulated. The alterations in the OM did not affect the ability of the mutant to grow in complex media, since the growth curves were not statistically different from those of the wild-type strain. The *gne*-deficient mutant lacked O antigen but contained the capsular polysaccharide. In fact, cells visualized in the micrographs were surrounded by ruthenium red-stained material and developed colonies with an opaque morphotype on agar plates. The *gne*-deficient mutant produces deficient-LPS, probably because the O-polysaccharide chain contains GlcNAc residues in each of its repeated units, like *A. hydrophila* serotype 034 (12) or *Yersinia enterocolitica* serotype 0:8 (7). This sugar was previously found in the capsule of the type strain of the species, which is a biotype 1 strain(22). The capsule of VSE strains does not seem to contain this sugar since the *gne*-deficient strain is a capsulated strain. In fact, at least 13 different K antigens have been described in the species (24).

Mutation in the *gne* gene of *V. vulnificus* VSE strains deeply affected the virulence phenotype of this zoonotic serovar. Eel vibriosis is a septicemic process comprising two steps: gill colonization and blood invasion with subsequent colonization of the internal organs (37, 56). The wild-type strain resisted the bactericidal action of gill mucus, was strongly attracted by it, and formed biofilms on mucus-coated plates, which correlates with its natural route of infection. In contrast, the *gne*-deficient mutant, although resistant to and chemoattracted by gill mucus, showed a significantly reduced ability to form biofilms on mucus compared with the wild-type strain. The translucent variant, which lacks most of the capsular material and retains the O antigen, formed as much biofilm on gill mucus as the wild-type strain. This result suggests that the O antigen rather than the capsule is involved in gill colonization, probably by facilitating attachment and biofilm formation on gills. Similar functions have been reported for the O antigen in *Vibrio cholerae*, since O-antigen-deficient *V. cholerae* strains are also deficient in mucus colonization (39).

The reduced motility observed in the *gne*-deficient mutant on semisolid surfaces seems not to be due to the loss of the flagellum or to defective flagellar biogenesis, since cells were motile in liquid medium and had a flagellum that was apparently the same length as the flagellum of the wild-type strain. Instead, the reduced swarming and swimming could be explained by the loss of a negatively charged O antigen, which would reduce the surface "wetability" required for colony expansion, as described previously for O-antigen-deficient mutants of *S. enterica* serovar Typhimurium (54).

It has been hypothesized that resistance to the innate defenses of the eel is the key step for colonization of the internal medium and death by septicemia (56). *V. vulnificus* VSE strains can survive in eel serum and resist the killing mechanisms of eel phagocytes in vitro, and spontaneous alterations in capsule and LPS that affect serum resistance have been described (2, 5). The *gne*-deficient mutant was sensitive to fresh eel serum and phagocytosis/opsonophagocytosis. The translucent spontaneous variant, which retains the O antigen and lacks most of the capsule, resisted the bactericidal action of eel serum; how-

ever, it grew significantly less than the wild-type strain and also resisted phagocytosis/opsonophagocytosis. Both strains fixed significantly more eel complement than the wild-type strain, especially when complement was activated by the classical pathway. These results suggest that the capsule and the O antigen may interfere with the deposition of natural antibodies and/or lectins on their natural targets (LPS core and other targets). The *gne*-deficient mutant was still sensitive to serum after inactivation by heating, which suggests that the loss of the O antigen makes the bacterium sensitive to a thermoresistant component naturally present in fresh serum or secreted by eel phagocytes. This extreme sensitivity to both eel serum and killing by phagocytes was correlated with a high level of sensitivity to cationic peptides present in eel serum and secreted by eel phagocytes (40), especially sensitivity to polymyxin B, which was significantly higher than the sensitivity of the translucent variant. The *gne*-deficient mutant was avirulent for eels, while the translucent variant was virulent for eels but exhibited a significantly higher LD_{50} than the wild-type strain. Thus, the resistance to the innate defenses of eels was well correlated to the degree of virulence for eels.

To evaluate the role of *gne* gene in human virulence, additional experiments to examine survival in human serum and virulence for mice were performed. Previous studies suggested that capsule was essential for human serum resistance by VSE cells and for virulence for mice (5). The results obtained in the present work confirm the previous findings since the translucent variant was sensitive to human serum and showed attenuated virulence for mice. As expected, the *gne*-deficient mutant was sensitive to human complement, even after heating, and showed attenuated virulence for mice, which confirms the role of the O antigen in resistance to both human and fish sera, as well as in virulence for both hosts. All these virulence traits were rescued by complementation of a mutant with the single gene *gne*.

Currently, eel vibriosis is kept under control on fish farms by vaccination by immersion with Vulnivaccine, a conventional bacterin that provides protection against vibriosis for 6 to 12 months (20). However, this vaccine and vaccination procedure do not eliminate the pathogen, which can survive on the eel surface inside biofilms (56), making the healthy carrier eels a risk to human health. The *gne*-deficient mutant is avirulent for fish and probably avirulent for humans since it was sensitive to human serum and showed attenuated virulence for mice, and at the same time, it can grow efficiently in complex media. This mutant could be a good candidate for development of a new live vaccine against eel vibriosis, at least against the disease caused by *V. vulnificu*s VSE strains.

In conclusion, *gne* plays an essential role both in O-antigen biosynthesis of the LPS and in virulence for humans and eels of VSE cells, whereas *galE* does not play a role in either OM biosynthesis or virulence. Further studies are under way to develop and validate a new live vaccine against fish vibriosis using the *gne*-deficient mutant, which could also prevent zoonosis caused by *V. vulnificus* VSE strains.

ACKNOWLEDGMENTS

This work was financed by projects MTKD-CT-2004-0145019 (European Union), AGL2005-04688 (Spanish Ministry for Education), PET2005-0053 (Spanish Ministry for Education), ACOMP07/063 (Generalitat Valenciana), and FIS (Spanish Ministry for Education and Science and Ministry of Healthcare and Generalitat de Catalunya). Esmeralda Valiente thanks the Spanish Ministry for Education, Culture and Sport for a Ph.D. fellowship, and Natalia Jimenez thanks the Generalitat de Catalunya for a Ph.D. fellowship.

We thank Maite Polo for her technical assistance and the SCIE of the University of Valencia for technical assistance with microscopy. The English was revised by F. Barraclough and James D. Oliver of the University of North Carolina.

REFERENCES

1. **Altschul, S. F., T. L. Madden, A. A. Schäffer, J. Zhang, Z. Zhang, W. Miller, and D. J. Lipman.** 1997. Gapped BLAST and PSI-BLAST: a new generation of protein database search programs. Nucleic Acids Res. **25:**3389–3402.
2. **Amaro, C., B. Fouz, E. G. Biosca, E. Marco-Noales, and R. Collado.** 1997. The lipopolysaccharide O side chain of *Vibrio vulnificus* serogroup E is a virulent determinant for eels. Infect. Immun. **65:**2475–2479.
3. **Amaro, C., and E. G. Biosca.** 1996. *Vibrio vulnificus* biotype 2, pathogenic for eels, is also an opportunistic pathogen for humans. Appl. Environ. Microbiol. **62:**1454–1457.
4. **Amaro, C., E. G. Biosca, B. Fouz, A. E. Toranzo, and E. Garay.** 1992. Electrophoretic analysis of heterogeneous lipopolysaccharides from various strains of *Vibrio vulnificus* biotypes 1 and 2 using silver staining and inmunoblotting. Curr. Microbiol. **25:**99–104.
5. **Amaro, C., E. G. Biosca, B. Fouz, A. E. Toranzo, and E. Garay.** 1994. Role of iron, capsule, and toxins in the pathogenicity of *Vibrio vulnificus* biotype 2 for mice Infect. Immun. **62:**759–763.
6. **Amaro, C., E. G. Biosca, B. Fouz, C. Esteve, and E. Alcalde.** 1995. Evidence that water transmits *Vibrio vulnificus* serovar E infections to eels. Appl. Environ. Microbiol. **61:**1133–1137.
7. **Bengoechea, J. A., E. Pinta, T. Salminen, C. Oertelt, O. Holst, J. Radziejewska-Lebrecht, Z. Piotrowska-Seget, R. Venho, and M. Skurnik.** 2002. Functional characterization of Gne (UDP-N-acetylglucosamine-4-epimerase), Wzz (chain length determinant), and Wzy (O-antigen polymerase) of *Yersinia enterocolitica* serotype O:8. J. Bacteriol. **184:**4277–4287.
8. **Bernatchez, S., C. M. Szymanski, N. Ishiyama, J. Li, H. C. Jarrell, P. C. Lau, A. M. Berghuis, N. M. Young, and W. W. Wakarchuk.** 2005. A single bifunctional UDP-GlcNAc/Glc-4 epimerase supports the synthesis of three cell surface glycoconjugates in *Campylobacter jejuni*. J. Biol. Chem. **280:**4792–4802.
9. **Biosca, E. G., E. Garay, A. E. Toranzo, and C. Amaro.** 1993. Comparison of the outer membrane protein profiles of *Vibrio vulnificus* biotypes 1 and 2. FEMS Microbiol. Lett. **107:**217–222.
10. **Biosca, E. G., H. Llorens, E. Garay, and C. Amaro.** 1993. Presence of a capsule in *Vibrio vulnificus* biotype 2 and its relationship to virulence for eels. Infect. Immun. **61:**1611–1618.
11. **Bisharat, N., V. Agmon, R. Finkelstein, R. Raz, G. Ben-Dror, L. Lerner, S. Soboh, R. Colodner, D. N. Cameron, et al.** 1999. Clinical, epidemiological, and microbiological features of *Vibrio vulnificus* biogroup 3 causing outbreaks of wound infection and bacteraemia in Israel. Israel Vibrio Study Group. Lancet **354:**1421–1424.
12. **Canals, R., N. Jiménez, S. Vilches, M. Regué, S. Merino, and J. M. Tomás.** 2007. Role of Gne and GalE in the Virulence of *Aeromonas hydrophila* serotype O34. J. Bacteriol. **189:**540–550.
13. **Carlton, B. C., and B. J. Brown.** 1981. Gene mutation, p. 224–225. *In* P. Gerhardt, R. G. E. Murray, R. N. Costilow, E. W. Nester, W. A. Wood, N. R. Krieg, and G. B. Phillips (ed.), Manual of methods for general bacteriology. American Society for Microbiology, Washington, DC.
14. **Castro, R., N. Couso, A. Obach, and J. Lamas.** 1999. Effect of different β-glucans on the respiratory burst of turbot (*Psetta maxima*) and gilthead seabream (*Sparus aurata*) phagocytes. Fish Shellfish Immunol. **9:**529–541.
15. **Chen, C. Y., K. M. Wu, Y. C. Chang, H. C. Tsai, T. L. Liao, Y. M Liu, A. B. Shen, J. C. Li, T. L. Su, C. P. Shao, C. T. Lee, L. I. Hor, and S. F. Tsai.** 2003. Comparative genome analysis of *Vibrio vulnificus*, a marine pathogen. Genome Res. **13:**2577–2587.
16. **Chen, Y., P. Bystricky, J. Adeyeye, P. Panigrahi, A. Ali, J. A Johnson, C. A. Bush, J. G. Morris, Jr., and O. C. Stine.** 2007. The capsule polysaccharide structure and biogenesis for non-O1 *Vibrio cholerae* NRT36S: genes are embedded in the LPS region. BMC Microbiol. **7:**20.
17. **Creuzenet, C., M. Belanger, W. Wakarchuk, and J. S. Lam.** 2000. Expression, purification and biochemical characterization of WbpP, a new UDP-GlcNAc C4 epimerase from *Pseudomonas aeruginosa* serotype O6. J. Biol. Chem. **275:**19060–19067.
18. **Esteve-Gassent, M. D., B. Fouz, R. Barrera, and C. Amaro.** 2004. Efficacy of oral immunisation after immersion vaccination against *Vibrio vulnificus* in farmed European eels. Aquaculture **231:**9–22.
19. **Fouz, B., and C. Amaro.** 2003. Isolation of a new serovar of *Vibrio vulnificus* pathogenic for eels cultured in freshwater farms. Aquaculture **217:**677–682.
20. **Fouz, B., M. D. Esteve-Gassent, R. Barrera, J. L. Larsen, M. E. Nielsen, and C. Amaro.** 2001. Field testing of a vaccine against eel diseases caused by *Vibrio vulnificus*. Dis. Aquat. Org. **45:**183–189.

21. **Fouz, B., F. Roig, and C. Amaro.** 2007. Phenotypic and genotypic characterization of a new fish-virulent *Vibrio vulnificus* serovar that lacks potential to infect humans. Microbiology **153:**1926–1934.
22. **Gunawardena, S., G. P. Reddy, Y. Wang, V. S. Kolli, R. Orlando, J. G. Morris, and C. A. Bush.** 1998. Structure of a muramic acid containing capsular polysaccharide from the pathogenic strain of *Vibrio vulnificus* ATCC 27562. Carbohydr. Res. **309:**65–76.
23. **Hanahan, D.** 1983. Studies on transformation of *Escherichia coli* with plasmids. J. Mol. Biol. **166:**557–580.
24. **Hayat, U., G. P. Reddy, C. A. Bush, J. A. Johnson, A. C. Wright, and J. G. Morris.** 1993. Capsular types of *Vibrio vulnificus*: an analysis of strains from clinical and environmental sources. J. Infect. Dis. **168:**758–762.
25. **Hitchcock, P. J., and T. M. Brown.** 1983. Morphological heterogeneity among *Salmonella* lipopolysaccharide chemotypes in silver-stained polyacrylamide gels. J. Bacteriol. **154:**269–277.
26. **Hoben. J., and P. Somasegaran.** 1982. Comparison of pour, spread, and drop plate methods for enumeration of *Rhizobium* spp. in inoculants made from presterilized peat. Appl. Environ. Microbiol. **44:**1246–1247.
27. **Ishikawaa, J., and K. Hotta.** 1999. Frameplot: a new implementation of the frame analysis for predicting protein-coding regions in bacterial DNA with a high G+C content. FEMS Microbiol. Lett. **174:**251–253.
28. **Kim, C. M., R. Y. Park, J. H. Park, H. Y. Sun, Y. H. Bai, P. Y. Ryu, S. Y. Kim, J. H. Rhee, and S. H. Shin.** 2006. *Vibrio vulnificus* vulnibactin, but not metalloprotease VvpE, is essentially required for iron-uptake from human holotransferrin. Biol. Pharm. Bull. **29:**911–918.
29. **Kim, Y. R., S. E. Lee, C. M. Kim, S. Y. Kim, E. K. Shin, D. H. Shin, S. S. Chung, H. E. Chey, A. Progulske-Fox, J. D. Hillman, M. Handfield, and J. H. Rhee.** 2003. Characterization and pathogenic significance of *Vibrio vulnificus* antigens preferentially expressed in septicemic patients. Infect. Immun. **71:** 5461–5471.
30. **Laemmli, U. K.** 1970. Cleavage of structural proteins during the assembly of the head of bacteriophage T4. Nature **227:**680–685.
31. **Larsen, M. H., J. L. Larsen, and J. E. Olsen.** 2001. Chemotaxis of *Vibrio anguillarum* to fish mucus: role of the origin of the fish mucus, the fish species and the serogroup of the pathogen. FEMS Microbiol. Ecol. **38:**77–80.
32. **Lee, C. T., C. Amaro, E. Sanjuan, and L. I. Hor.** 2005. Identification of DNA sequences specific for *Vibrio vulnificus* biotype 2 strains by suppression subtractive hybridization. Appl. Environ. Microbiol. **71:**5593–5597.
33. **Lindahl, M., A. Faris, T. Wadstrom, and S. Hjerten.** 1981. A new test based on "salting out" to measure relative surface hydrophobicity of bacterial cells. Biochim. Biophys. Acta **677:**471–476.
34. **Liu, P. V.** 1957. Survey of hemolysin production among species of pseudomonads. J. Bacteriol. **74:**718–722.
35. **Lowry, O., N. J. Rosebrough, A. L. Farr, and R. J. Randall.** 1951. Protein measurement with the Folin phenol reagent. J. Biol. Chem. **193:**265–275.
36. **Magre, S., Y. Takeuchi, G. Langford, A. Richards, C. Patience, and R. Weiss.** 2004. Reduced sensitivity to human serum inactivation of enveloped viruses produced by pig cells transgenic for human CD55 or deficient for the galactosyl-α(1-3) galactosyl epitope. J. Virol. **78:**5812–5819.
37. **Marco-Noales, E., M. Milan, B. Fouz, E. Sanjuán, and C. Amaro.** 2001. Transmission to eels, portals of entry, and putative reservoirs of *Vibrio vulnificus* serovar E (biotype 2). Appl. Environ. Microbiol. **67:**4717–4725.
38. **Martin, S. J., and R. J. Siebeling.** 1991. Identification of *Vibrio vulnificus* O serovars with antilipopolysaccharide monoclonal antibody. J. Clin. Microbiol. **29:**1684–1688.
39. **Nesper, J., S. Schild, C. M. Lauriano, A. Kraiss, K. E. Klose, and J. Reidl.** 2002. Role of *Vibrio cholerae* O139 surface polysaccharides in intestinal colonization. Infect. Immun. **70:**5990–5996.
40. **Nielsen, M. E., and M. D. Esteve-Gassent.** 2006. The eel immune system: present knowledge and the need for research. J. Fish Dis. **29:**65–78.
41. **Oliver, J. D.** 2006. *Vibrio vulnificus*, p. 349–366. *In* F. L. Thompson, B. Austin, and J. Swings (ed.), The biology of vibrios. ASM Press, Washington, DC.
42. **Oliver, J. D., and R. R. Colwell.** 1973. Extractable lipids of gram-negative marine bacteria: phospholipid composition. J. Bacteriol. **114:**897–908.
43. **Ørskov, F., and I. Ørskov.** 1978. Serotyping of Enterobacteriaceae with special emphasis on K antigen determination. Methods Microbiol. vol. **11:** 37–38.
44. **O'Toole, G. A., and R. Kolter.** 1998. Initiation of biofilm formation in *Pseudomonas fluorescens* WCS365 proceeds via multiple, convergent signalling pathways: a genetic analysis. Mol. Microbiol. **28:**449–461.
45. **Page, R. D. N.** 1996. TREEVIEW: an application to display phylogenetic trees on personal computers. Comput. Applic. Biosci. **12:**357–358.
46. **Park, N. Y., J. H. Lee, B. C. Lee, T. S. Kim, and S. H. Choi.** 2006. Identification and characterization of the *wbpO* gene essential for lipopolysaccharide synthesis in *Vibrio vulnificus*. J. Microbiol. Biotechnol. **16:**808–816.
47. **Park, N. Y., J. H. Lee, M. W. Kim, H. G. Jeong, B. C. Lee, T. S. Kim, and S. H. Choi.** 2006. Identification of the *Vibrio vulnificus wbpP* gene and evaluation of its role in virulence. Infect. Immun. **74:**721–728.
48. **Reed, M. J., and M. Muench.** 1938. A simple method for estimating fifty percent endpoints. Am. J. Hyg. **27:**487–493.
49. **Rubirés, X., F. Saigí, N. Piqué, N. Climent, S. Merino, S. Albertí, J. M. Tomás, and M. Regué.** 1997. A gene (*wbbL*) from *Serratia marcescens* N28b (024) complements the *rfb-50* mutation of *Escherichia coli* K-12 derivatives. J. Bacteriol. **179:**7581–7586.
50. **Sambrook, J., E. F. Fritsch, and T. Maniatis.** 1989. Molecular cloning: a laboratory manual, 2nd ed. Cold Spring Harbor Laboratory, Cold Spring Harbor, NY.
51. **Sanjuan, E., and C. Amaro.** 2007. Multiplex PCR assay for detection of *Vibrio vulnificus* biotype 2 and simultaneous discrimination of serovar E. Appl. Environ. Microbiol. **73:**2029–2032.
52. **Solem, S. T., J. B. Jørgensen, and B. Robertsen.** 1995. Stimulation of respiratory burst and phagocytic activity in Atlantic salmon (*Salmo salar* L.) macrophages by lipopolysaccharide. Fish Shellfish Immunol. **5:**475–491.
53. **Tison, D. L., M. Nishibuchi, J. D. Greenwood, and R. J. Seidler.** 1982. *Vibrio vulnificus* biogroup 2: new biogroup pathogenic for eels. Appl. Environ. Microbiol. **44:**640–646.
54. **Toguchi, A., M. Siano, M. Burkart, and R. M. Harshey.** 2000. Genetics of swarming motility in *Salmonella enterica* serovar Typhimurium: critical role for lipopolysaccharide. J. Bacteriol. **182:**6308–6321.
55. **Towbin, H., T. Staehelin, and T. Gordon.** 1979. Electrophoretic transfer of proteins from polyacrylamide gels to nitrocellulose sheets: procedure and some applications. Proc. Natl. Acad. Sci. USA **76:**4350–4354.
56. **Valiente, E., and C. Amaro.** 2006. A method to diagnose the carrier state of *Vibrio vulnificus* serovar E in eels. Aquaculture **258:**173–179.
57. **Wang, L., S. Huskic, A. Cisterne, D. Rothemund, and P. R. Reeves.** 2002. The O-antigen gene cluster of *Escherichia coli* O55:H7 and identification of a new UDP-GlcNAc C4 epimerase gene. J. Bacteriol. **184:**2620–2625.
58. **Wright, A. C., J. G. Morris, D. R. Maneval, K. Richardson, and J. B. Kaper.** 1990. Phenotypic evaluation of acapsular transposon mutants of *Vibrio vulnificus*. Infect. Immun. **58:**1769–1773.
59. **Wright, A. C., J. L. Powell, J. B. Kaper, and J. Glenn Morris.** 2001. Identification of a group 1-like capsular polysaccharide operon for *Vibrio vulnificus*. Infect. Immun. **69:**6893–6901.
60. **Yano, T.** 1992. Assays of hemolytic complement activity, p. 131–141. *In* J. S. Stolen, T. C. Fletcher, D. P. Anderson, S. L. Kaatari, and A. F. Rowley (ed.), Techniques in fish immunology. SOS Publications, New York, NY.
61. **Yu, H. B., P. S. Srinivasa Rao, H. C. Lee, S. Vilches, S. Merino, J. M. Tomás, and K. Y. Leung.** 2004. A type III secretion system is required for *Aeromonas hydrophila* AH-1 pathogenesis. Infect. Immun. **72:**1248–1256.

Editor: B. A. McCormick